Scheme I[a]

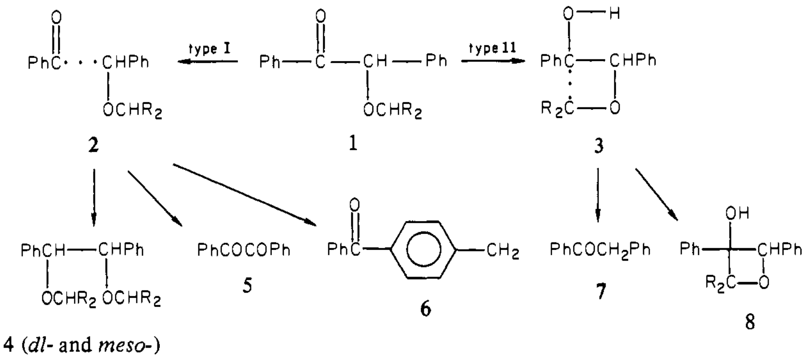

[a] a, R = H; b, R = Me.

Table I. Product Distribution in the Photolysis of 1a,b in MeOH and on Silica Gel with Temperature (mol % of Product Based on Starting Material Consumed)[a-c]

		type I			type II	
system	T, °C	4	5	6	7	8
1a–MeOH[d]	+56	43.7	8.6	5.7	3.3	2.4
	+4	39.6	16.7	3.9	1.0	1.8
	−51	38.1	20.3	3.6	0.4	0.7
	−78	29.9	14.2	3.6	0	0.3
1a–silica gel[e]	+56	43.8	3.0	6.7	13.0	3.1
	+4	30.0	3.8	7.1	4.6	3.3
	−55	25.7	7.2	38.3	9.8	8.9
	−78	10.8	2.5	39.6	6.2	6.0
1b–MeOH[d]	+56	40.7	5.0	12.8	2.9	1.4
	+11	44.9	13.9	8.7	1.2	0
	−44	47.1	23.6	9.1	0	0
	−80	44.7	25.2	18.3	0	0
1b–silica gel[e]	+56	39.4	1.6	10.2	10.2	3.9
	+12	38.2	10.6	16.5	10.6	6.8
	−40	18.1	8.2	35.8	11.5	14.7
	−78	6.8	6.4	58.3	13.4	20.2

[a] New compounds were characterized spectroscopically and mass spectroscopically. Compound 8a was synthesised. [b] Analysis by GC with docosane as an internal standard. [c] Silica gel irradiations were performed on degassed samples in horizontal rotating cylinders in front of a 500-W medium-pressure mercury arc, λ >300 nm. Conversion: 14–36%. [d] 0.18 mmol in 10 mL of MeOH. [e] Ca. 0.18 mmol on 3.0 g of silica gel (Merck 60, 35–70 mesh); approximately 5–10% coverage.

With **1a**, at room temperature, the amount of type II reaction (**7a** + **8a**) is considerably increased over that found in methanolic solution. On lowering the temperature the pinacol ethers (**4a**) become minor products, and the rearranged radical pair combination product **6a** becomes major, the proportions being essentially reversed. This is interpreted as an indication of the suppression of translational motion in the radical pairs **2a**[3b] but not of their rotational motion.

In addition to the increase in the type II process over that found in solution, the proportion of cyclization (of **3a**) to cleavage (**8a**:**7a**) is higher than that expected for a conformationally mobile system[16] that can assume either of the planar conformations necessary for cleavage.[10,11] This argues for a cisoid, but nonplanar, stereochemistry for **3a** when hydrogen bonded to the silica gel surface.

With **1b** the contrast between solution reaction and that on the silica gel surface is deepened. At 56 °C in both systems the results are comparable except for an increased amount, on silica gel, of type II reaction, mainly cleavage. At −78 °C the nongeminate pair combination **4b** has decreased to a sixth, whereas the rearranged geminate pair combination has increased 6-fold, to 58%. Again, translational, but not rotational, movement has been suppressed. The type II biradical is also being formed in increasing amount (33% of **7b** + **8b**) with cyclization dominating its subsequent behavior.

The results here reported are a consequence of two separate functions of the silica gel on the reacting species: conformational control and restricted movement. These are expected to be found acting independently and to have generality.

Acknowledgment. We thank the donors of the Petroleum Research Fund, administered by the American Chemical Society, and the National Science and Engineering Research Council of Canada for partial support.

Registry No. Benzoin methyl ether, 3524-62-7; benzoin isopropyl ether, 6652-28-4; silica, 7631-86-9.

---

(15) The ketones were deposited on the silica gel by removing the solvent from a dry methylene chloride slurry under 10^{-5} mmHg.

(16) Evidence was found, from variable-temperature ^{1}H NMR studies of **1b**, to be reported elsewhere, of slow (on the NMR time scale) rotation about the central bond, which cannot compete with the fast α cleavage.[5] The ether **1a** can do so more effectively.

Stable Gold Hydride Complexes

H. Lehner, D. Matt, P. S. Pregosin, and L. M. Venanzi*

Laboratorium für Anorganische Chemie
ETH-Zürich, CH-8092 Switzerland

A. Albinati

Istituto di Chimica Farmaceutica, Università di Milano
I-20131 Milano, Italy

Received June 18, 1982

No solid gold hydride species appear to be known,[1] although a monomeric gold hydride AuH has been detected in the gas phase.[2] Our previous studies on bridging hydride complexes[3] have shown that unstable mononuclear hydrides can be stabilized by complex formation to a second transition-metal center, e.g., $[(PEt_3)_2Pt(\mu\text{-}H)_2PtR(PEt_3)_2]BPh_4$ (R = H and Ph)[4] and $[(\text{diphos})Rh(\mu\text{-}H)_2IrH_2(P\text{-}i\text{-}Pr_3)_2]$.[5] We have, therefore, attempted the preparation of stable complexes containing Au–H bonds by formation of species of the type $LAuHML'_n$ by the reaction of an $(AuL)^+$ cation with a neutral metal hydride $(MH_mL'_n)$.

The compounds $[AuCl(PR_3)]$ (**1**, **a**, R = Ph; **b**, R = Et) react with $AgBF_4$ in THF to give the solvated cations [Au(THF)-

---

(1) Puddephatt, R. J. "The Chemistry of Gold"; Elsevier: Amsterdam, 1978. Since the submission of this paper some biheterometallic compounds of Au with Cr, Mo, or W have been reported, see: Green, M.; Orpen, A. G.; Salter, I. D.; Stone, F. G. A. *J. Chem. Soc., Chem. Commun.* **1982**, 813.

(2) Ringström, U. *Nature* (*London*) **1963**, *198*, 918.

(3) Venanzi, L. M. *Coord. Chem. Rev.* **1982**, *43*, 251 and references quoted therein.

(4) Bracher, G.; Grove, D. M.; Pregosin, P. S.; Venanzi, L. M. *Angew. Chem., Int. Ed. Engl.* **1979**, *18*, 155.

(5) Musco, A.; Naegeli, R.; Venanzi, L. M.; Albinati, A. *J. Organomet. Chem.* **1982**, *228*, C15.

(6) This reaction also gives an iridium hydride complex whose structure is, as yet, unknown.

0002-7863/82/1504-6825$01.25/0

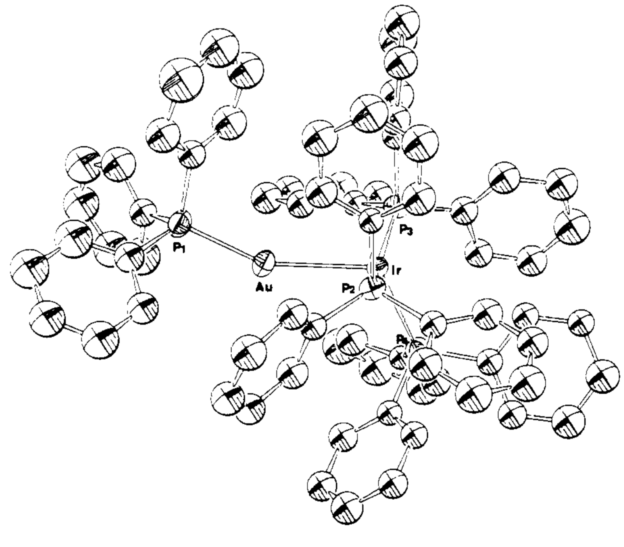

Figure 1. ORTEP drawing of the cation **4a**.

$(PR_3)]^+$ (**2**). Addition of these cations to THF solutions of *mer*-$[IrH_3(PPh_3)_3]$ (**3**) affords the binuclear cations **4**.

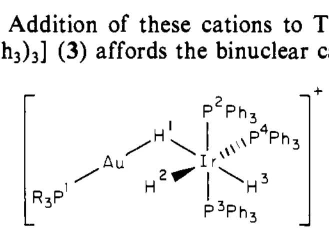

4a, R = Ph
b, R = Et

The related gold–platinum binuclear species, **5**, is obtained from the reaction of **2b** with *trans*-$[PtH(C_6Cl_5)(PEt_3)_2]$ (**6**).[7]

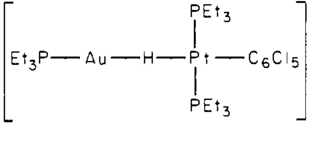

$$\left[Et_3P\text{—}Au\text{—}H\text{—}\overset{PEt_3}{\underset{PEt_3}{Pt}}\text{—}C_6Cl_5 \right]^+$$

5

Their combined ^1H and ^{31}P NMR spectra show unambiguously that the complexes are binuclear and that the bridging hydride ligand is bonded to both metal atoms. For **4a** the ^1H spectrum shows the three different hydride ligands at high field. The proton at δ −4.49, attributable to H^1, is coupled to the P^1 and P^4 atoms, as shown by selective $^1H\{^{31}P\}$ experiments, with the larger 79.4-Hz splitting assigned to $^2J_{^{31}P^1-^1H^1}$.[8] The $^{31}P\{^1H\}$ NMR spectrum of **4a** contains resonances at δ 48.2, 13.9, and 2.8, assignable to P^1, P^4, and P^2, respectively. The observation of a spin–spin coupling between P^1 and P^4, of 19.5 Hz, formally a four-bond interaction, provides additional support for the binuclear formulation. In the platinum complex, **5**, there is a single hydride proton resonance at δ −4.73, coupled to ^{195}Pt ($I = {}^1/_2$, natural abundance = 33.7%), $^1J_{^{195}Pt-^1H} = 537$ Hz, two equivalent phosphorus atoms on Pt, $^2J_{^{31}P-^1H} = 11$ Hz, and the single phosphorus coordinated to gold, $^2J_{^{31}P-^1H} = 78$ Hz. The latter spin–spin coupling is consistent with a trans orientation for these spins.[9] As with **4a**, the ^{31}P data confirm the binuclearity of the complex. The resonance for platinum-bound phosphorus, δ 13.7, is a singlet with ^{195}Pt satellites, $^1J_{^{195}Pt-^{31}P} = 2321$ Hz; moreover, the absorption for the gold-coordinated phosphorus at δ 43.7 also reveals ^{195}Pt satellites, $^3J_{^{195}Pt-^{31}P} = 274$ Hz, thereby connecting the phosphorus spin on gold to the second metal. The two types of P atoms are also spin coupled to each other, $^4J_{^{31}P-^{31}P} = 3$ Hz.

Table I. Some Selected Bond Lengths (Å) and Angles (Deg) for the Cation 4a[a] and for 3

	4a	3[11]
Au-Ir	2.765 (1)	
Au-P(1)	2.265 (5)	
Ir-P(2)	2.334 (6)	2.287 (3)
Ir-P(3)	2.325 (6)	2.285 (3)
Ir-P(4)	2.397 (4)	2.347 (3)
P-C	1.82 (2)[b]	
C-C	1.40 (4)	
Ir-Au-P(1)	155.3 (1)	
Au-Ir-P(2)	100.3 (1)	
Au-Ir-P(3)	87.4 (1)	
Au-Ir-P(4)	115.6 (1)	
P(2)-Ir-P(3)	149.9 (1)	153.0 (3)
P(2)-Ir-P(4)	100.0 (2)	102.8 (3)
P(3)-Ir-P(4)	102.7 (2)	101.6 (3)
P(1)-Au-Ir-P(2)	−68 (1)	
P(1)-Au-Ir-P(3)	82 (1)	
P(1)-Au-Ir-P(4)	−175 (1)	

[a] Estimated standard deviations on the last significant digit are given in parentheses. [b] Average value.

To extend our knowledge of the structural features of this class of compounds, we determined the single-crystal X-ray structure of **4a**.[10] The molecular structure is given in Figure 1, and some selected bond lengths and angles are given in Table I. The structure consists of an octahedral *mer*-$[IrH_3(PPh_3)_3]$ (**3**) unit bonded through the unique H atom to a $[Au(PPh_3)]^+$ cation. The coordination geometry at the iridium center is very similar to that found for mononuclear **3**[11] (see Table I). The most pronounced difference between **4a** and **3** is the lengthening of all the Ir–P bonds in the former relative to the latter.

The Ir–Au distance at 2.765 (1) Å is rather short, i.e., it is comparable with the M–M distance in compounds containing two bridging hydrides, e.g., $[(PEt_3)_2Pt(\mu\text{-}H)_2IrH_2(PEt_3)_2]BPh_4$,[12] 2.680 (1) Å, but shorter than that found in compounds having only one bridging hydride ligand, e.g., $[(PEt_3)_2(Ph)Pt(\mu\text{-}H)PtH(PEt_3)_2]BPh_4$, 3.09 (1) Å.[13] The most striking structural feature of **4a** is the Ir–Au–P bond angle, 155.34 (3)°. This arrangement is indicative of a bent M–H–M′ skeleton. Further, it should be noted that the dihedral angle defined by the atoms P^1–Au–Ir–P^4 is −175°, i.e., an almost all trans arrangement.

Although no X-ray structural data are available for **4b** or **5**, the NMR data suggest analogous structures for these compounds, and we assume this is also the case in the solid state. Thus, it would appear that complexes containing gold–hydrogen bonds can

---

(7) Carmona, D.; Thouvenot, R.; Venanzi, L. M., submitted for publication in *J. Organomet. Chem.*

(8) Additional ^1H and ^{31}P data for **4a**: $^2J_{P^4-H^1} = 11$ Hz (smaller coupling constants to P^2, H^2, and H^3 not resolved); δ −9.25 (H^2, $^2J_{P^4-H^2} = 101$ Hz, $^2J_{P^2-H^2} = 18$ Hz, $^4J_{P^1-H^2} = 13$ Hz), −11.19 (H^3, complex m, $^2J_{P^2-P^4} = 17.1$ Hz).

(9) Jesson, J. P. In "Transition Metal Hydrides"; Marcel Dekker, New York, 1971; p 75.

(10) A crystal of (**4a**)BF_4 was chosen for the X-ray analysis. Crystals are unstable in air and in the absence of solvent. Compound (**4a**)BF_4 ($C_{73}H_{65}AuIrP_4BF_4Cl_2$, M_r 1613.09) crystallizes in the triclinic space group $P\bar{1}$, with $a = 17.482$ (5) Å, $b = 15.617$ (5) Å, $c = 13.218$ (4) Å, $\alpha = 91.9$ (2)°, $\beta = 71.4$ (2)°, $\gamma = 103.9$ (3)° (least-squares-refined values obtained from 20 high-order reflections measured on an automatic diffractometer); $Z = 2$, $V = 33.12.9$ (4) Å^3; $\rho_c = 1.617$ g cm^{-3}. Data were collected on a Philips PW 1100 diffractometer up to a $2\theta_{max} < 38.0°$ at room temperature (Mo K$\bar{\alpha}$ graphite monochromated radiation) by using an $\omega/2\theta$ scan (scan width 1.40°, scan speed 0.08° s^{-1}); 4560 independent reflections were collected, of which 3792 were considered as observed ($I > 3\sigma(I)$) and subsequently used. The structure was solved by a combination of Patterson and Fourier methods and refined by block-diagonal least-squares analysis to the present conventional R factor of 0.054 (for the observed reflection) by using anisotropic thermal factors for Au, Ir, and P atoms and isotropic for the others; a correction for the real part of the anomalous dispersion has been allowed for. Scattering factors were taken from the "International Tables for X-ray Crystallography", Vol. IV. At the last stage of the refinement, a clathrated molecule of CH_2Cl_2 was located in the cell.

(11) Clark, G. R.; Skelton, B. W.; Waters, T. N. *Inorg. Chim. Acta* **1975**, *12*, 235.

(12) Boron, P.; Musco, A.; Venanzi, L. M. *Inorg. Chem.*, in press. Albinati, A., private communication.

(13) Bracher, G.; Grove, D. M.; Venanzi, L. M.; Bachechi, F.; Mura, P.; Zambonelli, L. *Angew. Chem., Int. Ed. Engl.* **1978**, *17*, 778.

indeed be stabilized by the interaction with a second transition-metal center.

A more complete account of the synthetic and crystallographic details will appear at a later date.

Acknowledgment is made to the Swiss National Science Foundation for support of this research.

Registry No. 1a, 14243-64-2; **1b**, 15529-90-5; **2a**, 83527-78-0; **2b**, 83527-79-1; **3**, 18660-47-4; **4a**, 83527-81-5; **4b**, 83527-83-7; **5**, 83527-85-9; **6**, 83527-86-0.

Supplementary Material Available: Positional parameters and thermal factors for the cation $[(PPh_3)Au(\mu\text{-}H)IrH_2(PPh_3)_3]^+$ (3 pages). Ordering information is given on any current masthead page.

Hemispherands Containing Cyclic Urea and Anisyl Units[1]

Donald J. Cram,* Ira B. Dicker, George M. Lein,
Carolyn B. Knobler, and Kenneth N. Trueblood

Department of Chemistry and Biochemistry
University of California, Los Angeles
Los Angeles, California 90024

Received July 12, 1982

Previous papers demonstrated that the spherands owe their superior alkali metal ion binding and selecting properties to the presence in the hosts prior to complexation of enforced cavities lined with electron pairs.[2] Crystal structure determinations demonstrated that the cavities of chorands and cryptands are filled with inward turned methylene groups that must be displaced by incoming ions during complexation.[3] Hemispherands are hosts at least half of whose cavity structures are organized for complexation during synthesis rather than during complexation. We report here the syntheses and binding properties of hemispherands **2–6** (Chart I) and the crystal structures of **4** and its $t\text{-BuNH}_3ClO_4$ complex. Because of their awkward names, hosts **1–6** and their precursors are referred to by combinations of letters, each of which stands for a binding unit. The code is indicated and is illustrated by the sequence $A(AD)_2D$ for **1** (Chart I), whose synthesis, binding properties,[4] and crystal structure (and that of its $t\text{-BuNH}_3^+$ complex) have been reported.[3] The syntheses of **2–6** are outlined in the supplementary material. All new compounds gave elemental analyses within 0.30% of theory and ^1H NMR and mass spectra compatible with their assigned structures.

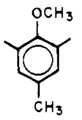
A

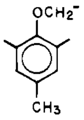
A'

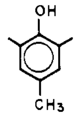
Ah

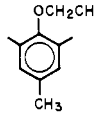
Aa

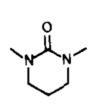
U

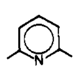
P

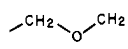
D

Chart I

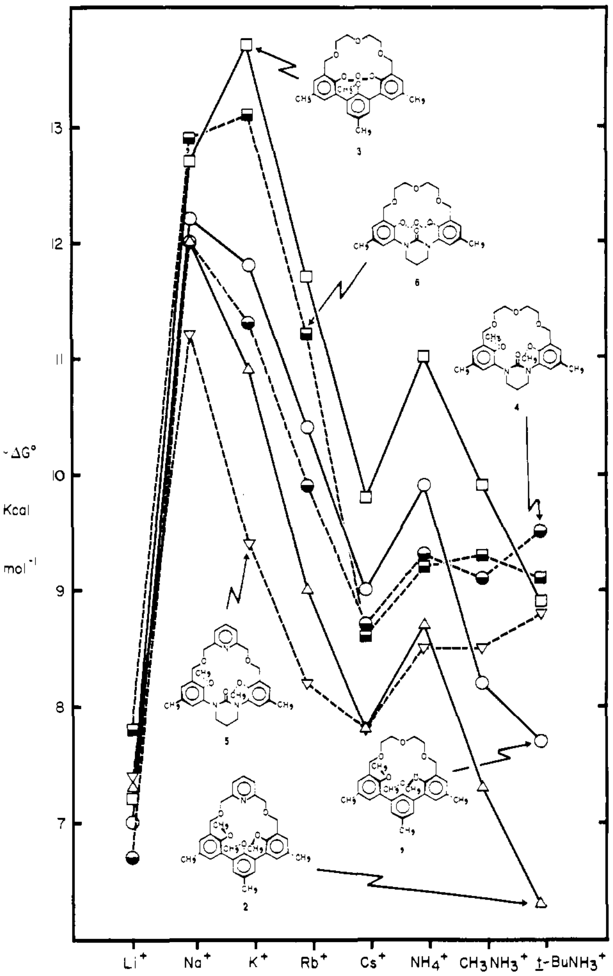

Drawing **7** depicts the preliminary crystal structure of free host $U(AD)_2D$ (**4**), and **8** that of its complex, $U(AD)_2D\cdot t\text{-BuNH}_3^+$. Notice that the A–U–A units in **7** and **8** possess essentially the same organization. The two anisyl oxygens are on the side of the macroring opposite to that of the urea oxygen, and the unshared electron pairs of the three oxygens line a half cavity. In the free host **7**, the unshared electron pairs of the three oxygens of the D–D–D unit diverge from the cavity, which is filled with inward-turned hydrogens of two CH_2 groups, as is observed in the crystal structures of numerous chorands.[3] Upon complexation, these hydrogens are displaced from the cavity, and the unshared electron pairs of the three oxygens in the complex converge on the cavity. Thus some organizational burden with respect to the *chorand part* of the host is placed on the guest during complexation, as has been observed with $A(AD)_2D$ (**1**) complexing $t\text{-BuNH}_3^+$.[3] As expected from CPK molecular model examination of $U(AD)_2D\cdot t\text{-BuNH}_3^+$ prior to its synthesis, the $t\text{-BuNH}_3^+$ group hydrogen bonds the urea and the two benzyloxy oxygens in a tripod arrangement to provide the perching complex indicated in **8**. This tripod binding is possible only when the guest occupies that face of the macroring that is anti to the oxygens of the two anisyl units. The opposite face is occupied in the $A(AD)_2D\cdot t\text{-BuNH}_3^+$ complex.[3] As expected, in **8** the C–C–N–H dihedral angles are close to 60°, and this C–N bond is essentially normal to the plane of the three hydrogen-bonded oxygens.

The $t\text{-BuNH}_3^+ClO_4^-$ complexes in $CDCl_3$ solution of $U(AD)_2D$ (**4**), $U(AD)_2P$ (**5**), and $A'(U)(D)(DDD)A'$ (**6**) must resemble each other since in their ^1H NMR spectra, the signals of the guests' CH_3 groups are moved upfield to δ 0.644, 0.503, and 0.78, respectively. Model examination of all three complexes indicate the CH_3 groups are located in the shielding cones of two or three aryl groups. In contrast, for the $t\text{-BuNH}_3^+$ complex of $A(AD)_2D$

---

[1] We thank the Division of Basic Sciences of the Department of Energy for the contract (AT(04-3), P.A. 218) that supported all of the research except the crystal structure work, for which we thank the National Science Foundation, Grant NSF CHE 80-22525.

[2] (a) Cram, D. J.; Lein, G. M.; Kaneda, T.; Helgeson, R. C.; Knobler, C. B.; Maverick, E.; Trueblood, K. N. *J. Am. Chem. Soc.* **1981**, *103*, 6228–6232. (b) Lein, G. M.; Cram, D. J. *J. Chem. Soc., Chem. Commun.* **1982**, 301–304.

[3] Cram, D. J.; Trueblood, K. N. *Top. Curr. Chem.* **1981**, *98*, 43–106.

[4] Koenig, K.; Lein, G. M.; Stückler, P.; Kaneda, T.; Cram, D. J. *J. Am. Chem. Soc.* **1979**, *101*, 3553–3566.